



Molecular and Cellular Life Sciences: Infectious Diseases, Biochemistry and Structural Biology  
2015 Conference, MCLS 2015

## Mutation Analysis of the $pK_a$ Modulator Residue in $\beta$ -D-xylosidase from *Geobacillus thermoleovorans* IT-08: Activity Adaptation to Alkaline and High-Temperature Conditions

Lanny Hartanti<sup>a,e</sup>, Ali Rohman<sup>b</sup>, Ami Suwandi<sup>e</sup>, Bauke W. Dijkstra<sup>c</sup>, Zeily Nurahman<sup>d</sup>, Ni Nyoman Tri Puspaningsih<sup>a,b,\*</sup>

<sup>a</sup>Proteomic Laboratory of Institute of Tropical Diseases, Universitas Airlangga, Kampus C Mulyorejo, Surabaya 60115, Indonesia

<sup>b</sup>Department of Chemistry, Faculty of Sciences and Technology, Universitas Airlangga, Kampus C Mulyorejo, Surabaya 60115, Indonesia

<sup>c</sup>Laboratory of Biophysical Chemistry, University of Groningen, Nijenborgh 7, 9747 AG Groningen, the Netherlands

<sup>d</sup>Biochemistry Division, Faculty of Mathematics and Natural Sciences, Institut Teknologi Bandung, Jl. Ganesha 10, Bandung 40132, Indonesia

<sup>e</sup>Faculty of Pharmacy, Widya Mandala Catholic University, Jl. Kalisari Selatan 1, Surabaya 60112, Indonesia

### Abstract

$\beta$ -D-xylosidases are hemicellulases that catalyze the release of xylose units from short xylooligosaccharides. Their activity is the rate-limiting step in xylan hydrolysis. A major application of these enzymes is as eco-friendly biobleaching agents in the pulp and paper industry, where thermostable, alkaliphilic xylosidases are much preferred. Hence, the isolation and characterization of new thermo-alkaliphilic xylosidases from nature, or re-engineering existing ones is of importance for industrial applications. The thermophilic bacterium *Geobacillus thermoleovorans* IT-08 produces a meso-thermophilic  $\beta$ -D-xylosidase (EC 3.2.1.37), which has a unique primary structure compared to other xylosidases with only 32-35% amino acid sequence identity. Here, we describe the role of Asp121 in modulating the enzyme's pH-activity profile. Mutation of this residue into Val121 or Asn121 increased its pH optimum by 3 pH units with a significant decrease in its activities. Furthermore, all mutants showed a significant 40 °C increase in optimum temperature compared to wild-type enzyme. This study thus illustrates the importance of the  $pK_a$  modulator residue Asp121 in shifting the pH- and temperature-activity profile of the enzyme. Changing Asp/Asn residues in enzymes, especially when the residue is located near the catalytic site, may be a useful strategy for adapting the enzyme to a high pH and high temperature environment.

© 2016 The Authors. Published by Elsevier B.V. This is an open access article under the CC BY-NC-ND license

(<http://creativecommons.org/licenses/by-nc-nd/4.0/>).

Peer-review under responsibility of the organizing committee of the Molecular and Cellular Life Sciences: Infectious Diseases, Biochemistry and Structural Biology 2015 (MCLS 2015)

**Keywords:**  $\beta$ -D-xylosidase; *Geobacillus thermoleovorans* IT-08; pH optimum, temperature optimum; site-directed mutagenesis;  $pK_a$  modulator

\* Corresponding author. Tel.: +62-811-345-2009; fax: -.

E-mail address: [nyomantri@yahoo.com](mailto:nyomantri@yahoo.com); [nyomantri@unair.ac.id](mailto:nyomantri@unair.ac.id)

## Nomenclature

GbtXyl43A	$\beta$ -D-xylosidase from <i>Geobacillus thermoleovorans</i> IT-08
D121V	mutant of GbtXyl43A, Asp121 mutated to Val121
D121E	mutant of GbtXyl43A, Asp121 mutated to Glu121
D121N	mutant of GbtXyl43A, Asp121 mutated to Asn121
pNP-X	pNP- $\beta$ -D-xylopyranoside
pNP	para-nitrophenol

## 1. Introduction

Xylan is the major hemicellulosic polysaccharide in plant cell walls and the second most abundant renewable polysaccharide in nature<sup>1</sup>. As a potentially renewable energy resource that may be converted into biofuel, xylan hydrolysis has gained growing interest. Xylan is a heterogeneous polysaccharide composed of a  $\beta$ -1,4-linked xylopyranosyl backbone substituted with different side chains such as arabinofuranose, methylglucuronic acid and acetate. Owing to its complex structure, complete degradation of xylan requires the concerted action of several hemicellulolytic enzymes. The main enzymes involved in xylan hydrolysis are endo-1,4- $\beta$ -xylanases (EC 3.2.1.8), which hydrolyze the xylan backbone into  $\beta$ -D-xylopyranosyl oligosaccharides, and  $\beta$ -D-xylosidases (EC 3.2.1.37), which further degrade the resulting xylo-oligosaccharides to free xylose<sup>2</sup>.

One of the major current applications of xylanases is in the pulp and paper industry, since hydrolysis of xylan by these enzymes facilitates the release of lignin from paper pulp and allows to reduce the amount of hazardous chlorine as bleaching agent, and also results in better pulp brightness<sup>3,4</sup>. Most industrial pulping is done at high temperature (55-70°C) and under alkaline conditions, hence requiring xylanases to be operationally stable under such conditions<sup>5,6,7</sup>. Alkaliphilic xylanases are also required for detergent applications where typically high pHs are used<sup>8</sup>. Considering the nature of industrial applications, generating xylanases that are more active and stable at alkaline conditions would help to reduce process costs.

Various pretreatments are commonly applied to lignocellulosic biomass prior to enzymatic hydrolysis to fractionate, solubilize, hydrolyze and separate cellulose, hemicellulose and lignin components. The treatment strategies solubilize hemicelluloses and degrade it to a mixture of xylo-oligosaccharides that need to be further hydrolyzed in order to be used by microorganisms for production of fuel ethanol and chemicals.  $\beta$ -D-xylosidase in this respect is very helpful to hydrolyze the xylo-oligosaccharides to simple sugars<sup>9</sup>.

$\beta$ -D-xylosidase activity is the rate-limiting step in xylan hydrolysis, and thus supplementary  $\beta$ -D-xylosidase is usually added to commercial hemicellulolytic enzyme mixtures to boost xylan hydrolysis<sup>10</sup>. For instance, the extent of xylan hydrolysis increased from 18% to 48% when *Neurospora crassa*  $\beta$ -xylanase was supplemented with *N. crassa*  $\beta$ -xylosidase<sup>11</sup>. Other industrial applications of microbial  $\beta$ -D-xylosidases are in the baking industry, production of animal feed, D-xylose production for xylitol manufacturing, de-inking of recycled paper, and hydrolysis of lignocellulosic biomass in biofuel fermentations to produce ethanol and butanol<sup>12</sup>.

The  $\beta$ -D-xylosidase from *Geobacillus thermoleovorans* IT-08 belongs to glycoside hydrolase family 43 and is optimally active at 55°C, when assayed at pH 6.0<sup>13</sup>. The  $\beta$ -D-xylosidase gene (GBTXYL43A; GenBank accession No. [DQ345777](#)) has been successfully subcloned into the pET101/D-TOPO expression vector (Puspaningsih, unpublished work). Compared to several other members of the GH43  $\beta$ -D-xylosidase family deposited in the Protein Data Bank with 52-67% amino acid sequence identity among each other<sup>13</sup>, the sequence of GbtXyl43A is more divergent, with an identity of 33.5% to the nearest structurally characterized homologue, i.e. the  $\beta$ -1,4-xylosidase from *Bacillus halodurans* C-125 (PDB code 1YRZ<sup>14</sup>). In view of its evolutionary divergence, we consider it of interest to explore the structure-functional properties of this enzyme. Herein, we describe the engineering of GbtXyl43A to replace the residue that was identified as potentially influencing the pH-activity profile of the enzyme based on structural modeling and inspection of a model of the active site with the aim of increasing its pH optimum.

## 2. Methods

### 2.1. Strains, growth conditions and reagents

*Escherichia coli* TOP10 was used for all plasmid constructions while *E. coli* BL21 (DE3) was used for all protein expressions. Conditions for over-production and purification of all enzymes in this study were as outlined previously<sup>13</sup>. Growth media were purchased from Becton, Dickinson and Company (France), and unless otherwise stated all other chemical reagents were purchased from Sigma-Aldrich (Switzerland).

### 2.2. Selecting residues for site-directed mutagenesis

A model of the three-dimensional structure of  $\beta$ -D-xylosidase from *Geobacillus thermoleovorans* IT-08 (GbtXyl43A) was generated using the on-line program SWISS-MODEL (<http://swissmodel.expasy.org><sup>15</sup>) based on the coordinates of 1YRZ chain B<sup>14</sup>. This model was used to identify residues that were potentially in a position to interact with the catalytic residues and that could be reasonably expected to regulate the protonation or deprotonation of the residues involved in catalysis. The model was evaluated by the Swiss-PDB viewer/DeepView program<sup>16</sup>. Asp121 was identified as the residue closest to the two catalytic residues, and was therefore chosen as target for mutation, replacing it with Asn, Glu and Val. Models of the mutant enzymes were generated using the Swiss-PDB Viewer.

### 2.3. Evaluation of mutant enzymes models

Models of mutant enzymes were evaluated on the basis of their physical and chemical characteristics (theoretical pI, instability index, aliphatic index, molecular weight, total of negative and positive residues) by the *online* program ProtParam (<http://web.expasy.org/protparam/>). The modeled three-dimensional structures of the mutant proteins were energy-minimized using GROMOS 96 as implemented in the Swiss-PdbViewer before further analysis.

### 2.4. Mutant construction

Isolation of recombinant  $\beta$ -D-xylosidase plasmids was done using the QIAprep Spin Miniprep Kit (Qiagen) according to the manufacturer's protocol. Site directed mutagenesis was performed using Platinum *Taq* DNA polymerase High Fidelity (Invitrogen) and primers from First Base (Singapore). Primers were designed with the CloneManager program (Scientific & Educational Software, 2000), based on the  $\beta$ -D-xylosidase DNA sequence from GenBank (GenPept ABC75004). The primers used are listed in Table S1 of the Supplementary data. The PCR amplification step consisted of 25 cycles of denaturation at 95°C for 30 s, annealing for 50 s at 51-61°C (according to the  $T_m$  of the used primers, Table S1), and 3 minutes extension at 72°C. A final extension was carried out for 5 minutes at 72°C. The PCR was carried out using a GeneAmp PCR System 2400 (Perkin Elmer, Mount Holy, NJ, USA). After the polymerase chain reaction, the products were subjected to DpnI (Fermentas) digestion to remove template DNA and then transformed into *E. coli* TOP10. The mutations were confirmed by nucleotide sequencing analysis. The verified plasmids were isolated and transformed into *E. coli* BL21 (DE3) for protein overexpression.

### 2.5. Expression and purification of proteins

Procedures for expression of GbtXyl43A in recombinant *E. coli* strain BL21 (DE3) containing the pET-*xyl* plasmid and its purification have been established<sup>13</sup>. In brief, an overnight pre-culture of the recombinant *E. coli* was grown in LB (Luria-Bertani) medium supplemented with 100  $\mu$ g/mL ampicillin. This pre-culture was used for 1% inoculation of 1 L fresh LB medium containing 100  $\mu$ g/mL ampicillin. Expression of GbtXyl43A was induced with 1 mM of isopropyl- $\beta$ -D-1-thiogalactopyranoside (IPTG) at an OD<sub>600</sub> of 0.7-0.8 and the *E. coli* cells were harvested after an additional 3 hours of growth. Following cell lysis, GbtXyl43A was heated to 323 K for 1 h and centrifuged to remove the *E. coli* insoluble proteins caused by heating. Purification of GbtXyl43A was continued with immobilized Ni<sup>2+</sup>-affinity chromatography (HisTrap HP; GE Healthcare) and anion-exchange chromatography

(Resource Q; GE Healthcare) using an ÄKTAexplorer (GE Healthcare). The purified GbtXyl43A in storage buffer (25 mM Tris-HCl buffer, pH 8.0, and 100 mM NaCl) was concentrated to 14 mg mL<sup>-1</sup> using an Amicon Ultra-4 30K filter (Millipore) and freeze-stored at 253 K until usage. Protein concentrations were determined using the Bradford protein assay kit (Bio-Rad) with bovine serum albumin as a standard and its purity was monitored by Coomassie blue-stained SDS-PAGE. All mutant proteins were expressed and purified using the same procedures as the wild type protein.

### 2.6. Determination of enzyme activity at various temperatures and pHs

Activity assays of purified enzymes were performed using 2.0 M *p*NP-β-D-xylopyranoside (*p*NP-X, Sigma Chemical) as substrate at 40°C. The assay solution contained 450 μL substrate in modified universal buffer<sup>17</sup> of a certain pH and 50 μL enzyme, which were separately pre-incubated at 40°C for 10 minutes prior to the assay. After 30 minutes of incubation at 40°C, 50 μL of 0.4 M sodium carbonate solution was added to the mixture. The absorbance of liberated *p*NP was measured at 400 nm. Each assay was performed at least in triplicate. One unit of recombinant GbtXyl43A activity (IU) was defined as the amount of enzyme required to produce 1 μmol *p*NP per minute at reaction conditions.

The activities of recombinant GbtXyl43 and its mutants as a function of pH were assayed using the *p*NP-X substrate in modified universal buffer in the pH range 2.0–10.0, and incubating with enzyme solution at 40°C for 30 minutes. The optimum temperature was determined by assaying the enzyme activity at 30–90 °C. Each assay was performed in triplicate.

### 2.7. Crystallization of mutant proteins

All mutant proteins were crystallized at 283 K using the hanging-drop vapor-diffusion method at the same conditions as those previously described<sup>13</sup>. In a typical experiment, 1 μL of GbtXyl43A solution (7 mg mL<sup>-1</sup> in the storage buffer) was mixed with an equal volume of reservoir solution containing 0.1 M HEPES buffer, pH 7.0, and 5% (w/v) PEG 6000. Crystal formation was accelerated by streak seeding using available GbtXyl43A crystals as seeds. Under these conditions, two mutant proteins, *i.e.* D121E and D121V, yielded crystals overnight with dimensions of about 100 x 100 x 100 μm<sup>3</sup>.

### 2.8. X-ray data collection

Prior to the X-ray diffraction experiments, the crystals were cryoprotected by soaking them for 5 s into buffer containing 20% (v/v) glycerol, followed by flash-cooling them in liquid nitrogen. X-ray diffraction data sets for D121V and D121E crystals were collected at 100 K on beamline ID14-1 (European Synchrotron Radiation Facility, Grenoble) using an ADSC Quantum Q210 detector. All data sets comprised 330 frames with an oscillation range per frame of 0.3° and were processed using the programs XDS<sup>18</sup> and SCALA<sup>19</sup> from the CCP4 package<sup>20</sup>. A summary of the crystallographic data collection and processing can be found in Table 1.

## 3. Results and Discussion

### 3.1. Structural modeling of GbtXyl43A and selection of residues for mutation

Since the structure of the 508-residue GbtXyl43A has not been deposited in the protein data bank, we constructed a model to facilitate the selection of residues suitable for mutation. The model was constructed using the automated modeling mode of SWISS-MODE, in which the program automatically searches for structures of homologous proteins in the Protein Data Bank (PDB) (<http://www.rcsb.org>). The best modeling template found was the 2.0 Å resolution crystal structure of the xylan β-1,4-xylosidase from *Bacillus halodurans* C-125 with PDB entry 1YRZ chain B<sup>14</sup>, with a sequence identity of only 33.5% to GbtXyl43A (GenPept ABC75004.1). Despite the low homology, the modeled structure of GbtXyl43A has a good reliability estimate (QMEAN6 score 0.72, QMEAN6 Z-score - 0.59<sup>20</sup>).

Table 1. The summary of crystallographic data collection and processing (values in parentheses are for the outer shell resolution)

	Wild type <sup>13</sup>	D121V
Beamline	ID23-3, ESRF	ID14-1, ESRF
Detector	ADSC Quantum Q210	ADSC Quantum Q210
Wavelength (Å)	0.87260	0.93340
Resolution (Å)	1.55 (1.63–1.55)	2.00 (2.11–2.00)
Space group	<i>P</i> 4 <sub>3</sub> 2 <sub>1</sub> 2	<i>P</i> 4 <sub>3</sub> 2 <sub>1</sub> 2
Unit-cell parameters		
<i>a</i> = <i>b</i> (Å)	62.53	62.6
<i>c</i> (Å)	277.4	276.0
<i>α</i> = <i>β</i> = <i>γ</i> (°)	90	90
Molecules per asymmetric unit	1	1
Matthew's coefficient (Å <sup>3</sup> Da <sup>-1</sup> )		2.35
Solvent content (%)		47.7
<i>R</i> <sub>merge</sub> <sup>†</sup>	0.146 (0.761)	0.078 (0.132)
<i>R</i> <sub>p.i.m.</sub> <sup>‡</sup>	0.040 (0.280)	0.030 (0.051)
Total observations	1 150 089 (94 995)	297 178 (41 906)
Unique reflections	81 489 (11 687)	38 123 (5 382)
Mean <i>I</i> / <i>σI</i>	14.2 (2.3)	17.1 (10.2)
Completeness	100.0 (100.0)	99.8 (99.2)
Multiplicity	14.1 (8.1)	7.8 (7.8)

$$^{\dagger} R_{\text{merge}} = \frac{\sum_h \sum_i |I_i(h) - \langle I(h) \rangle|}{\sum_h \sum_i I_i(h)}$$

$$^{\ddagger} R_{\text{p.i.m.}} = \frac{\sum_h \left[ \frac{1}{(N-1)} \right]^{1/2} \sum_i |I_i(h) - \langle I(h) \rangle|}{\sum_h \sum_i I_i(h)}$$

*I*<sub>*i*</sub>(*h*) is the integrated intensity of a reflection,  $\langle I(h) \rangle$  is the mean intensity of multiple corresponding symmetry-related reflections, and *N* is the multiplicity of the given reflections.

As other GH43 family enzymes GbtXyl43A has two domains, an N terminal five-bladed β-propeller catalytic domain, and a β-sandwich domain<sup>22</sup>. In GH43, hydrolysis of the substrate proceeds with inversion of the anomeric configuration *via* a single nucleophilic displacement<sup>13</sup>. The catalytic mechanism involves three catalytic residues, with Glu177 acting as general acid, Asp14 as general base, and Asp121 as the residue that modulates the p*K*<sub>a</sub> of the general acid and keeps it in the correct orientation relative to the substrate<sup>22</sup>. Analysis of the three-dimensional structure of GbtXyl43A with the Swiss-PDB Viewer revealed that several residues interact with the catalytic residues. These residues are Ala193 that forms 2 hydrogen bonds with Glu177, Ala178 that forms one hydrogen bond with Asp121, and Ser29 that form one hydrogen bond with Asp14 (Fig. 1).

Though there is no hydrogen bond formed between Glu177 and Asp121, the smallest distance between them (2.62 Å) is the closest compared to the distance of Glu177 and other residues. This explains the important role of Asp121 in enforcing that Glu177 is protonated at pH 6.0, the pH optimum, allowing Glu177 to function as the catalytic acid during the reaction. Changing Asp121 will change the charge distribution around Glu177, and thus may change the pH profile of the enzyme.

The importance of the p*K*<sub>a</sub> modulator residue in inverting GH43 β-xylosidases has been explained by Brüx *et al.*<sup>22</sup> for XynB3, the GH43 β-xylosidase from *G. stearothermophilus*. Besides modulating the p*K*<sub>a</sub> of the catalytic acid, the p*K*<sub>a</sub> modulator residue may also guide the catalytic acid into the correct orientation toward the substrate. It also plays an important role in substrate binding *via* the 2-O of the sugar bound in subsite-1, as the most important interaction for transition state stabilization of the substrate. Indeed, mutation of the residue into glycine (D128G) yielded a less active enzyme than the general acid mutant E187G. Considering the important roles of the p*K*<sub>a</sub> modulator residue in inverting GH43 β-xylosidases and the low 31.8% sequence identity of GbtXyl43A to XynB3, we decided to study the role of Asp121 in GbtXyl43A as a p*K*<sub>a</sub> modulator. Instead of mutation into glycine, as was done in XynB3, we mutated this residue into Asn, Glu and Val, in order to study the effect of the mutation on the pH-activity profile.

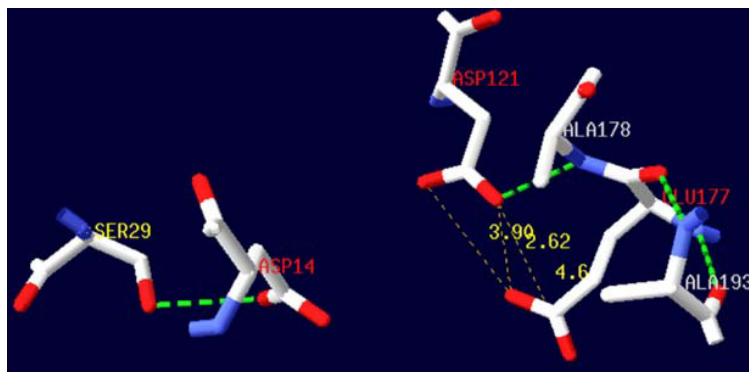


Fig. 1. The representation of catalytic residues in GbtXyl43 (red label) and its neighbours (grey label). The green dotted line represents hydrogen bond between adjacent residues. The yellow number shows the length of hydrogen bond, in Angstrom

### 3.2. GbtXyl43A and mutant proteins expression and purification

The  $\beta$ -D-xylosidase GbtXyl43A and all mutants were successfully expressed in *E. coli* BL21, and purified, as confirmed by SDS-gel analysis of the cell-lysate and eluate from the  $\text{Ni}^{2+}$ -NTA affinity column for the purification of the His-tagged protein. All purified proteins showed a high level of purity, with a molecular weight of around 58 kDa (Fig. 2). We found that GbtXyl43A and D121E were expressed in higher quantities than D121V and D121N. Similar expression levels have been reported by Yang *et al.*<sup>23</sup> for *Bacillus circulans* xylanase (BCX) and its mutants. Two BCX mutants, Q167M and R73V, showed lower expression compared to wild-type BCX and the K175Q mutant. Interestingly, the mutants with lower expression levels showed a pronounced alkaline shift in their pH-activity profiles, while the K175Q mutant showed a similar pH-activity profile as that of wild-type BCX. Thus, we expected that two mutants of GbtXyl43A, i.e. D121V and D121N, would also show significant changes in their pH-activity profiles compared to that of the wild-type enzyme.

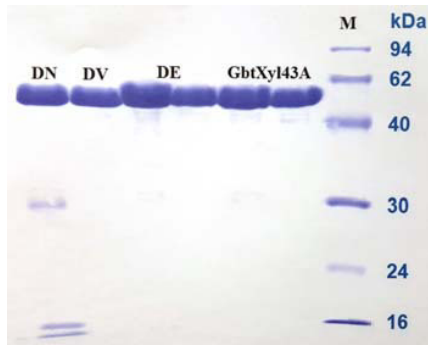


Fig. 2. SDS-PAGE purification profile of  $\beta$ -D-xylosidase GbtXyl43A and D121N (DN), D121V (DV) and D121E (DE) mutants, stained with Coomassie Blue; M = protein marker

### 3.3. pH-activity profile of GbtXyl43A and mutant proteins

The pH-activity profile of the mutants D121V, D121E and D121N were determined and compared to that of the GbtXyl43A wild-type enzyme (Fig. 3). All mutants showed a pH-activity profile that differed from that of the wild-type enzyme. Two mutants, D121V and D121N, showed a pronounced alkaline shift of their pH-activity. Their optimum activities had shifted to pH 9.0, 3 units above that of wild-type enzyme (pH 6.0). Unfortunately, their activities were much lower than that of the wild-type (about 5% and 3% respectively, for D121V and D121N). These results are in agreement with our prediction concerning the role of Asp121 as  $\text{pK}_a$  modulator in  $\beta$ -xylosidase. Although the importance of this residue for catalysis has previously been demonstrated<sup>22</sup>, its importance for the pH-optimum had not yet been explored.



Asparagine is a polar, non-charged amino acid. DeepView analysis of the mutant model predicted that the change of a carboxylate into a carboxamide function introduces a new hydrogen bond from  $\text{HN}^{\delta 2}$  of Asn121 to  $\text{O}^{\epsilon 1}$  of Glu177. The length of hydrogen bond formed is 1.5 Å. Though the interaction between these two residues is closer, but since the electronegativity of N is smaller than O, the capability of  $\text{N}^{\delta 2}$  of Asn121 in donating its proton to  $\text{O}^{\epsilon 1}$  of Glu177 is also smaller. Consequently, to be able to function as an acid in the catalytic reaction, Glu177 needs proton donation from the environment, in other words the pH optimum of the enzyme will be shifted to a more alkaline range.

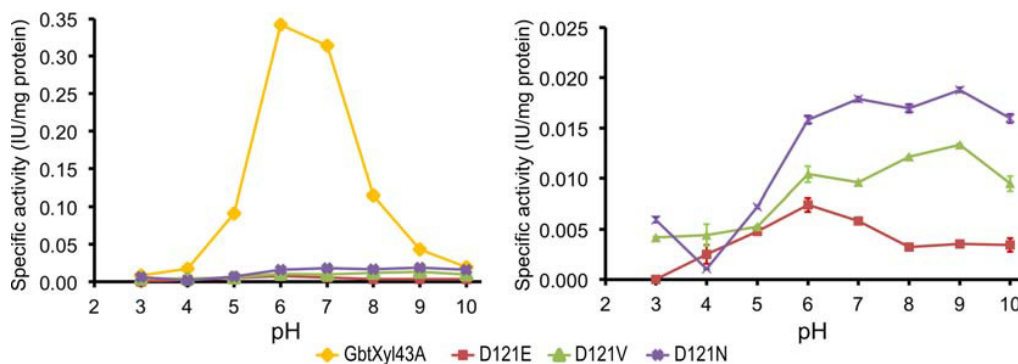


Fig.3. Activity profile for GbtXyl43A (◆); D121E (■); D121N (▲); and D121E (X) in various pHs, the right curve is the enlargement scale for pH-activity profile for D121E (■); D121N (▲); and D121E (X). Activity assays were conducted with substrate 2.0 mM *p*NP-β-D-xylopyranoside (*p*NPX) at 50 °C for 30 min. Each assay was done in duplicate. Xylosidase specific activity is defined as the amount of *p*-nitrophenol liberated each minute on certain temperature and pH for each mg protein

Mutation of Asp121 into Val121 also shifted the optimum pH of GbtXyl43A into a more alkaline range. As a non-polar amino acid, valine contains no oxygen or other electronegative atom and has a high hydrophobicity degree. This makes the protonation of Glu177 by valine impossible. Moreover since valine only has a short side chain, thus the distance between Val121 and Glu177 was bigger compared to that of Asp121 and Glu177. Consequently valine was unable to protonate  $\text{O}^{\epsilon 1}$  of Glu177 and hence shifted the pH optimum of GbtXyl43A into a more alkaline range.

Glutamate, on the other hand, is a negative-polar charged amino acid. Compared to aspartate, glutamate has one more carbon in its side chain that made the overall distance to Glu177 closer than the wild-type. Thus, protonation of Glu177 was easier in D121E and hence slightly shifted the optimum pH of GbtXyl43A into a more acid range. The activity of D121E was much lower than that of the wild-type. We assume that this was caused by the additional torsion angle of the glutamate side chain compared to Asp. In the wild-type enzyme the  $\text{O}^{\delta 2}$  of aspartate is held in position by a hydrogen bond with the main chain N of Ala178, providing the exact orientation required for stabilizing the protonated state of Glu177. The loss of this hydrogen-bonding interaction in D121E could cause the significant loss of activity. However, further investigation would be necessary to fully confirm these mechanisms, especially further structural studies on protein-substrate complex.

Overall, our results confirmed several other findings concerning the mechanism of acidic or alkaline pH catalytic adaptation. Study of acidophilic xylanase family 11 revealed the role of charged amino acid residues on the adaptation process. The carboxyl group near the glutamate catalytic residue is able to decrease or increase the  $\text{p}K_a$  value of the catalytic residue, in which the effect depends on the electrostatic bridges formed between the interacting residues<sup>6</sup>. In our case, this phenomenon was found in D121E mutant that showed a  $\text{p}K_a$  decreasing effect. In acidophilic xylanase of *Aspergillus kawachii*, mutation of aspartate that is hydrogen bonded to general acid/base catalytic residue into asparagine changed the activity of xylanase to a more alkaline condition, i.e. from pH 2.0 into pH 5.0<sup>6</sup>. Our mutant, D121N, also showed a 3 units optimum pH shift to alkaline condition. Other random mutagenesis experiment on xylanase from *Neocallimastix patriciarum* showed that increasing of negative charge and hydrophobicity could increase the optimum pH of enzyme<sup>6</sup>. Study of alkaline active xylanase of *Bacillus halodurans* S7 also underlined the role of charged residues in alkaline adaptation. Alkaline active xylanase have

highly acidic surfaces and fewer solvent exposed alkali labile residues<sup>7</sup>. Study of the low pH optimum mechanism in *A. niger* xylanase I also revealed that the Asp37 residue influences critically the pH dependence of activity. This residue is substituted for asparagine in all xylanases with a high pH optimum<sup>24</sup>. Contrary to that, mutation of Asp121 to Glu121 that supposed to increase the acidic surfaces of the catalytic site was unable to change GbtXyl43A into an alkaline active enzyme. On the other hand, we found that mutation of aspartate into valine could increase the hydrophobicity around catalytic residues, and hence increased the optimum pH of GbtXyl43A.

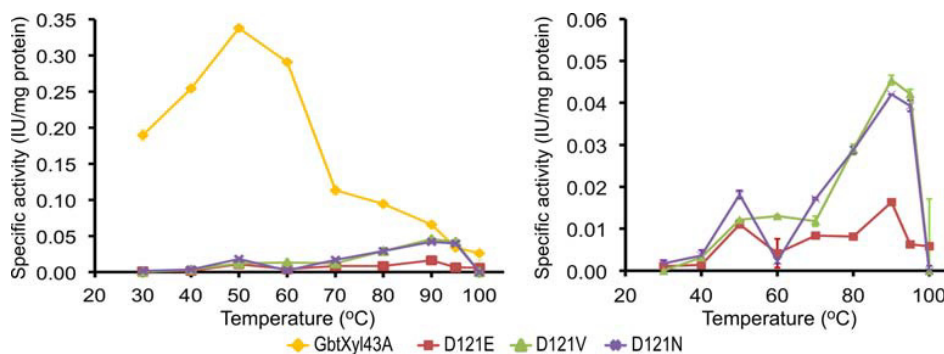


Fig. 4. Temperature-activity profile for GbtXyl43A (◆); D121E (■); D121N (▲); and D121V (×); the right curve is the enlargement scale for temperature activity profile for D121E (■); D121N (▲); and D121V (×). Activity assays were conducted for 30 min, in 2.0 mM *p*NPX pH 6 for GbtXyl43A and D121E or in 2.0 mM *p*NPX pH 9 for D121V and D121N. Each assay was done in duplicate. Xylosidase specific activity is defined as the amount of *p*-nitrophenol liberated each minute at certain temperature and pH for each mg protein

### 3.4. Temperature-activity profile of GbtXyl43A and mutants protein

Since Asp121 is one of the three catalytic residues in  $\beta$ -D-xylosidase, the dramatic reduction in activity caused by its mutation is reasonable. Interestingly, besides the shift in the pH-activity profile, mutation of Asp121 also shifted the temperature-activity profile (Fig. 4). All mutants showed a pronounced shift in its temperature optimums, 40°C higher than that of the wild type, i.e. at 90°C. However the mutation caused significantly loss in the activities. At the optimum temperature, D121E had activity of only 4.7% compared to GbtXyl43A activity at 50°C. On the other hand, mutant D121N and D121V showed a similar pattern in the temperature-activity profile at 30-100°C. Both mutants at the temperature optimum (90°C) had activities of 12.4% and 13.3% respectively, compared to the activity of GbtXyl43A at its temperature optimum (50°C). Thus the mutants D121V and D121N showed the pronounced effect on the temperature-activity profile. Several factors have been reported to contribute to protein stability at high temperature, such as increasing of hydrophobic or ionic interactions, increasing of proline content, reduction of the amount of thermolabile amino acid such as Cys or Asn, or increasing of disulfide bridges in cytoplasmic proteins<sup>24</sup>. Here we report that mutation of Asp into Asn and Val in GbtXyl43A could increase the optimum temperature of the enzyme. Though Asn is considered as the most thermolabile amino acid, but if the mutation was located in the catalytic site or at important residue in the catalysis process, the thermostability of the enzyme could be increased. Changing Asp into Asn and Val seemed to increase the hydrophobic interaction in the surface area of binding in the catalytic site, and thus increased the thermal stability of the protein.

### 3.5. Crystals structure of GbtXyl43A-mutants

Crystallization trials using hanging drop and seeding method only succeeded to crystallize two of three mutants. The condition applied in crystallization procedures was the same as the condition applied in GbtXyl43A-Wild Type crystallization, which used PEG 6000 solutions in 0.1 M HEPES buffer pH 7.0<sup>13</sup>. Tetragonal crystals of mutant D121V and D121E (Fig. 5a,b) grew within one night from 5% PEG 6000 after being seeded with GbtXyl43A crystal to a maximum dimension of 100 x 100 x 100  $\mu\text{m}^3$  and belong to space group  $P4_32_12$ .



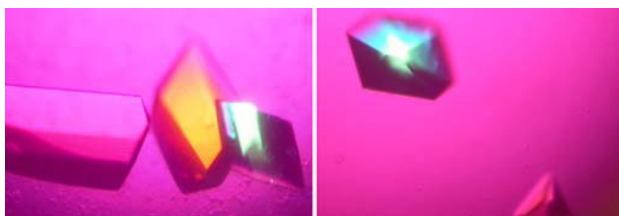


Fig. 5. Tetragonal crystals of GbtXyl43A-mutants; D121V (left) and D121E (right).

All crystals obtained could diffract X-rays as shown in Fig. 6, but only mutant D121V could give data collection statistics as shown in Table 1. The diffracted crystal of mutant D121E was in the form of a double crystal. Overall these results lead us to the conclusion that mutation of Asp121 into Glu and Val did not change the overall structure of the proteins a lot. Though Asp121 was buried in the center of the five-bladed  $\beta$ -propeller fold of the enzyme, its mutation into these three amino acid residues gave only a minor shift to its packing in crystal formation. Unlike other mutants generated in this study, mutant D121N was not able to be crystallized using the same conditions used to crystallize GbtXyl43A and its other mutants. The precipitant solution should be change since we have tried and not succeeded in crystallizing it using several PEG 6000 solution concentrations. This has revealed the importance of Asp121 to Asn121 mutation in  $\beta$ -xylosidase from *Geobacillus thermoleovorans* IT-08.

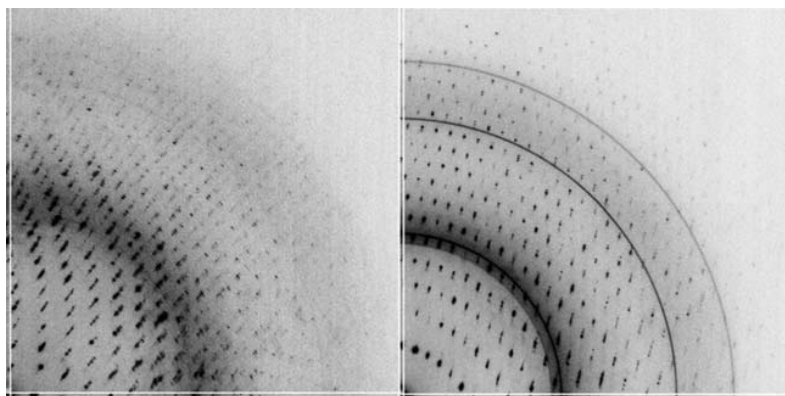


Fig. 6. X-ray diffraction images. A part of a frame recorded from of D121E (left panel, the resolution at the edge is 1.9 Å) and D121V (right panel, 1.7Å) GbtXyl43A crystals. See Table 1 for further information.

#### 4. Conclusion

The  $pK_a$  modulator is a conserved and crucial amino acid residue in all  $\beta$ -D-xylosidase family GH43 members. Though changing this residue reduced the activity dramatically, but certain mutation was proven to be a useful tool to engineer a more alkaline and thermoactive  $\beta$ -xylosidase. Mutation of Asp121 into Val121 and Asn121 of  $\beta$ -D-xylosidase from *Geobacillus thermoleovorans* IT-08 were able to shift the optimum pH into a more alkaline pH range and cause an increase in its optimum temperature. Our results revealed the importance of asparagines and valine residue located at or near the catalytic site of  $\beta$ -D-xylosidase family GH43 in its activity in alkaline and higher temperature condition.

#### Acknowledgements

This research was partially supported by the Directorate General of Higher Education, Ministry of Education and Culture, the Republic of Indonesia through Hibah Tim Pascasarjana scheme to N.N.T.P. (2011-2012), Sandwich Course Program 2011 to L.H., as well as Doctoral Scholarship Program to L.H. We thank Much Zaenal Fanani for his assistance in the production of enzymes at the Proteomic Laboratory of Institute of Tropical Diseases, Universitas Airlangga, Indonesia, and Dr. K. Muruga Poopathi Raja, Ph.D for a critical reading of the manuscript.

## Appendix A. Supplementary Data

Table S1. Sequence of Mutagenic Primers

Mutation	Code <sup>*)</sup>	Length (bp)	Primer sequences <sup>**)</sup>	T <sub>m</sub> (°C)	GC (%)
D121E	D121E-F	17	5'-GGAGGCATTGA <u>G</u> CCATC-3'	59.6	58.8
	D121E-R	17	5'-GATGGCTCAATGCCTCC-3'	59.6	58.8
D121N	D121N-F	19	5'-GATGGGGAGGCATT <u>A</u> ATCC-3'	60.2	52.6
	D121N-R	19	5'-GGAT <u>T</u> AATGCCTCCCCATC-3'	60.2	52.6
D121V	D121V-F	19	5'-GGAGGCATTG <u>T</u> TCCATCAC-3'	60.2	52.6
	D121V-R	19	5'-GTGATGGA <u>A</u> CAATGCCTCC-3'	60.2	52.6

<sup>\*)</sup> F code is forward primer, R code is reverse primer

<sup>\*\*)</sup> The mutational positions are shown as bold and underlined nucleotide residues

## References

- Coughlan, MP, Hazlewood, GP.  $\beta$ -1,4-Xylan-degrading enzyme systems: biochemistry, molecular biology and applications. *Biotechnol Appl Biochem* 1993; 17: 259–289.
- Bravman, T, Zolotnisky, G, Belakhov V, Shoham, G, Henrissat, B, Baasov, T, Shoham, Y. Detailed kinetic analysis of a family 52 glycoside hydrolase: a  $\beta$ -xylosidase from *Geobacillus stearothermophilus*. *Biochemistry* 2003; 42: 10528-36.
- Viikari, L, Kantelinen, A, Sundquist, J, Linko, M. Xylanases in bleaching: from an idea to the industry. *FEMS Microbiol Rev* 1994; 13: 335–350.
- Beg, QKM, Kapoor, L, Mahajan, G, Hoondal, S. Microbial Xylanase from the Newly Isolated Bacillus sp. Strain BP-23. *Can J Microbiol* 2001; 39: 1162-1166.
- Sarethy, IP, Saxena, Y, Kapoor, A, Sharma, M, Sharma, SK, Gupta, V, Gupta, S. Alkaliphilic bacteria: applications in industrial biotechnology. *J Ind Microbiol Biotechnol* 2011; 38: 769-790.
- Collins, T, Gerday, C, Feller, G. Xylanases, xylanase families and extremophilic xylanases. *FEMS Microbiol Rev* 2005; 29: 3-23.
- Mamo, G, Thunnissen, M, Hatti-Kaul, R, Mattiasson, B. An alkaline active xylanase: insights into mechanisms of high pH catalytic adaptation. *Biochimie* 2009; 91:1187-1196.
- Kumar, BK, Balakrishnan, H, Rele, MV. Compatibility of alkaline xylanases from an alkaliphilic Bacillus NCL (87-6-10) with commercial detergents and proteases. *J Ind Microbiol Biotechnol* 2004; 31(2): 83–87.
- Saha, BC. Purification and properties of an extracellular  $\beta$ -xylosidase from a newly isolated *Fusarium proliferatum*. *Biores Technol* 2003; 90: 33-38.
- Sørensen, HR, Meyer, AS, Pedersen, S. Enzymatic hydrolysis of water-soluble wheat arabinoxylan: Synergy between  $\alpha$ -L-arabinofuranosidases, endo-1,4- $\beta$ -xylanases, and  $\beta$ -xylosidase activities. *Biotechnol Bioeng* 2003; 81(6): 726-31.
- Han, Y, Chen, H. A  $\beta$ -xylosidase from cell wall of maize: Purification, properties and its use in hydrolysis of plant cell wall. *J Mol Catal B: Enzym* 2010; 63: 135-140.
- Jordan, DB, Wagschal, K. Properties and applications of microbial  $\beta$ -D-xylosidases featuring the catalytically efficient enzyme from *Selenomonas ruminantium*. *Appl Microbiol Biotechnol* 2010; 86(6): 1647-1658.
- Rohman, A, van Oosterwijk, N, Kralj, S, Dijkhuizen, L, Dijkstra, BW, Puspaningsih, NNT. Purification, crystallization and preliminary X-ray analysis of a thermostable glycoside hydrolase family 43  $\beta$ -xylosidase from *Geobacillus thermoleovorans* IT-08, *Acta Crystallogr* 2007; F63: 932-935.
- Arnold K., Bordoli L, Kopp J, Schwede T. The SWISS-MODEL Workspace: A web-based environment for protein structure homology modeling. *Bioinformatics* 2006; 22:195-201.
- Guex, N, Peitsch, MC. SWISS-MODEL and the Swiss-PdbViewer: An environment for comparative protein modeling. *Electrophoresis* 1997; 18: 2714-2723.
- Kabsch, W. XDS. *Acta Crystallogr* 2010; D66: 125-132.
- Turner, BL. Variation in pH optima of hydrolytic enzyme activities in tropical rain forest soils. *App Environ Microbiol* 2010; 76(19): 6485-6493.
- Evans, P. Scaling and assessment of data quality, *Acta Crystallogr* 2006; D62:72-82.
- Winn, MD, Ballard, CC, Cowtan, KD, Dodson, EJ, Emsley, P, Evans, PR, Keegan, RM, Krissinel, EB, Leslie, AGW, McCoy, A., McNicholas, SJ, Murshudov, GN, Panny, NS, Potterton, EA, Powell, HR, Read, RJ, Vagin, A., Wilson, KS. Overview of the CCP4 suite and current developments. *Acta Crystallogr* 2011; D67: 235-242 [ doi:10.1107/S0907444910045749 ]
- Benkert, P, Biasini, M, Schwede, T. Towards the estimation of the absolute quality of individual protein structure models. *Bioinformatics* 2011; 27(3): 343-350.
- Brüx, C, Ben-David, A, Shallom-Shezifi, D, Leon, M, Niefind, K, Shoham, G, Shoham, Y, Schomburg, D. The Structure of an Inverting GH43  $\beta$ -Xylosidase from *Geobacillus stearothermophilus* with its Substrate Reveals the Role of the Three Catalytic Residues. *J Mol Biol* 2006; 359: 97-109.
- Yang, JH, Park, JY, Kim, SH, Yoo, YJ. Shifting pH optimum of *Bacillus circulans* xylanase based on molecular modeling. *J Biotechnol* 2008; 133: 294-300.
- Krengel, U, Dijkstra, BW. Three-dimensional structure of endo-1,4- $\beta$ -xylanase I from *Aspergillus niger*: molecular basis for its low pH optimum. *J Mol Biol* 1996; 263: 70-78.
- Littlechild, JA, Guy, J, Connelly, S, Mallett, L, Waddell, S, Rye, CA, Line, K, Isupov, M. Natural methods of protein stabilization: thermostable biocatalysts. *Biochem Soc Trans* 2007; 35(6): 1558-1563.